Supplementary materials

Text S1. Tree-structured Parzen estimator optimization

All “single-site” and “all-sites” optimizations reached a convergence in the first 200 iterations (Fig. S1 and S2). The mean optimization cost substantially reduced after fluctuations in the first 100 trials, indicating the obvious advance toward finding the optimized PFT-V_{cmax25}. The fluctuations of the mean optimization cost in the first 100 trials also indicated that the optimizations were performed through extensive explorations of model performance.

Text S2. Global data products of gross primary production and evapotranspiration

We extracted stand-level estimates from various gridded global data products of gross primary production and evapotranspiration (Table 1). All the estimates employed here were evaluated over North America’s boreal biome in previous studies. We acknowledge that the gridded data products may be produced based on replicated observations (e.g., the MODIS products) and were not fully independent. However, we treated all data products as independent data because they were produced separately based on independent protocols.

Table S1. CLASSIC parameters for estimating the maximum carboxylation rate (V_{cmax}) from V_{cmax25} (V_{cmax} at 25 °C; μmol CO_2 m^{-2} s^{-1}). T_{lower} and T_{upper} (°C) are the lower and upper temperature thresholds for photosynthesis (Melton and Arora, 2016; Meyer et al., 2021).

Plant functional type	V_{cmax25}	T_{lower}	T_{upper}
Evergreen Needleleaf Tree (ENT)	42	-5	34
Deciduous Needleleaf Tree (DNT)	47	-5	34
Evergreen Broadleaf Shrub (EBS)	60	-2	34
Deciduous Broadleaf Shrub (DBS)	60	-2	34
C3 grass (C3G)	55	-1	40
Sedge (SDG)	40	-1	40

Table S2. Study boreal forest stands. 30-year climate normals of mean annual air temperature (MAAT) and mean annual total precipitation (MATP) (Qu et al., 2022). Site names refer to AmeriFlux ID and sites are in a latitudinal order from south (CA-Qfo) to north (CA-HPC). Permafrost is isolated (≤10 % in areal extent), sporadic (>10 – 50 %), discontinuous (>50 – 90 %), and continuous (>90 %).

Site (AmeriFlux-ID)	Name	Latitude	Longitude	MAAT	MATP	Permafrost
CA-Qfo	Quebec - Eastern Boreal, Mature Black Spruce	49.69	-74.34	0.2 ℃	929 mm	Absent
CA-Obs	Saskatchewan - Western Boreal, Mature Black Spruce	53.99	-105.12	1.1 ℃	474 mm	Absent
CA-Man	Manitoba - Northern Old Black Spruce (former BOREAS Northern Study Area)	55.88	-98.48	-1.7 ℃	324 mm	Absent
CA-SMC	Smith Creek	63.15	-123.25	-2.8 ℃	389 mm	Discontinuous
US-BZS	Bonanza Creek Black Spruce	64.70	-148.32	-2.0 ℃	280 mm	Discontinuous
US-Uaf	University of Alaska, Fairbanks	64.87	-147.86	-3.9 ℃,	367 mm	Discontinuous
US-Prr	Poker Flat Research Range Black Spruce Forest	65.12	-147.49	-2.9 ℃	391 mm	Discontinuous
CA-HPC	Havikpak Creek	68.32	-133.52	-6.8 ℃	235 mm	Continuous

Table S3. Maximum carboxylation rate at 25 °C (V_{cmax25}; μmol CO_2 m^{-2} s^{-1}) obtained from leaf-level gas exchange measurements (Sect. 2.4). Plant functional types (PFTs) are "evergreen needleleaf tree" (ENT), "deciduous needleleaf tree" (DNT), "evergreen broadleaf shrub" (EBS), "deciduous broadleaf shrub" (DBS), "C3 grass" (C3G), and "sedge" (SDG). An asterisk (*) indicates that the measurements were standardized to 25 °C using an Arrhenius function (Smith et al., 2019; Kattge and Knorr, 2007).

PFT	Plant species	V_{cmax25}	Measured periods	Location	Source
ENT	*Picea mariana*	46.5 ± 9.6	June–October	Balsam, MN, USA	Jensen et al. (2019)
ENT	*Picea mariana*	39.0 ± 6.4	July	Guelph, ON, CA	Smith and Dukes (2017)
ENT	*Picea mariana*	24.6 ± 4.0	July	Timmins, ON, CA	Smith and Dukes (2017)
ENT	*Picea mariana*	25.6 ± 8.8*	July	Prince Albert, SK, CA	Rayment et al. (2002)
ENT	*Picea mariana*	19.7 ± 5.3*	May–September	Nelson House, MB, CA	Dang et al. (1998)
ENT	*Picea mariana*	25.1 ± 3.8	July–August	Fort Greely, AK, USA	Ueyama et al. (2018)
ENT	*Picea mariana*	30.4 ± 8.6	August	Deltana, AK, USA	Smith and Dukes (2017)
ENT	*Picea mariana*	26.2 ± 9.6	July–August	Fairbanks, AK, USA	Ueyama et al. (2018)
ENT	*Pinus banksiana*	25.5 ± 6.1*	May–September	Nelson House, MB, CA	Dang et al. (1998)
DNT	*Larix laricina*	45.9 ± 29.2	June–October	Balsam, MN, USA	Jensen et al. (2019)
DNT	*Larix laricina*	38.3 ± 8.0	July	Guelph, ON, CA	Smith and Dukes (2017)
DNT	*Larix laricina*	33.4 ± 8.8	July	Timmins, ON, CA	Smith and Dukes (2017)
DNT	*Larix laricina*	42.8 ± 12.6	August	Deltana, AK, USA	Smith and Dukes (2017)
EBS	*Chamaedaphne calyculata*	43.2 ± 8.2	June–October	Balsam, MN, USA	Jensen et al. (2019)
EBS	*Rhododendron groenlandicum*	37.8 ± 2.8	June–October	Balsam, MN, USA	Jensen et al. (2019)
EBS	*Vaccinium myrtilloides*	84.6 ± 13.5	July–August	Wakefield, ON, CA	Bubier et al. (2011)
EBS	*Ledum groenlandicum*	78.1 ± 13.4	July–August	Wakefield, ON, CA	Bubier et al. (2011)
EBS	*Rhododendron ferrugineum*	35	May–September	Antras, OCC, FR	Pornon and Lamaze (2007)
EBS	*Ledum groenlandicum*	47.8 ± 16.8	July–August	Fairbanks, AK, USA	Ueyama et al. (2018)
DBS	*Kalmia polifolia*	67.7 ± 22.8	June–October	Balsam, MN, USA	Jensen et al. (2019)
DBS	*Vaccinium angustifolium*	36.3 ± 1.8	June–October	Balsam, MN, USA	Jensen et al. (2019)
DBS	*Vaccinium myrtillus*	20.7*	June–July	Cavedine, TN, IT	Wohlfahrt et al. (1999)
DBS	*Vaccinium uliginosum*	62*	June–July	Innsbruck, TR, AT	Wohlfahrt et al. (1999)
DBS	*Betula glandulosa*	58.3 ± 6.4	July–August	Fairbanks, AK, USA	Ueyama et al. (2018)
DBS	*Betula nana*	37.3 ± 9.3	June–July	Toolik lake, AK, USA	Heskel et al. (2013)

DBS	*Salix pulchra*	103.5	July–August	Barrow, AK, USA	Rogers et al. (2017)
SDG	*Eriophorum vaginatum*	20.0 ± 11.0	June–July	Toolik lake, AK, USA	Heskel et al. (2013)
SDG	*Carex aquatilis*	87.3	July–August	Barrow, AK, USA	Rogers et al. (2017)
SDG	*Eriophorum angustifolium*	71.9	July–August	Barrow, AK, USA	Rogers et al. (2017)
C3G	*Arctagrostis latifolia*	85.5	July–August	Barrow, AK, USA	Rogers et al. (2017)
C3G	*Arctophila fulva*	113	July–August	Barrow, AK, USA	Rogers et al. (2017)
C3G	*Dupontia fisheri*	69	July–August	Barrow, AK, USA	Rogers et al. (2017)

Table S4. Model performance (mean ± standard deviation) in root mean square deviation (RMSD) and Pearson correlation coefficient (r) using the prior and optimized plant functional type (PFT)-V_{cmax25} compared with eddy covariance observations of gross primary production (GPP) and evapotranspiration (ET). The units of RMSD are g C m^{-2} day^{-1} for GPP and mm day^{-1} for ET. Site names refer to AmeriFlux ID and sites are in a latitudinal order from south (CA-Qfo) to north (CA-HPC) (Table S2).

Flux	Statistical metrics	PFT-V_{cmax25}	CA-Qfo	CA-Obs	CA-Man	CA-SMC	US-BZS	US-Uaf	US-Prr	CA-HPC
GPP	RMSD	"single-site"	2.0 ± 1.3	1.9 ± 0.9	1.5 ± 0.6	1.9 ± 1.0	2.3 ± 1.6	2.9 ± 1.0	0.9 ± 0.4	2.5 ± 1.9
		"all-sites"	2.0 ± 1.3	1.9 ± 0.9	1.6 ± 0.7	2.1 ± 1.1	2.3 ± 1.1	2.9 ± 0.9	1.1 ± 0.4	2.6 ± 2.0
		prior	3.5	2.4	2	3.1	2.8	2.8	1.2	4.4
	r	"single-site"	0.89 ± 0.01	0.88 ± 0.01	0.88 ± 0.04	0.78 ± 0.01	0.93 ± 0.00	0.80 ± 0.03	0.90 ± 0.01	0.90 ± 0.01
		"all-sites"	0.88 ± 0.01	0.87 ± 0.02	0.88 ± 0.03	0.77 ± 0.02	0.93 ± 0.01	0.83 ± 0.02	0.89 ± 0.01	0.90 ± 0.01
		prior	0.87	0.86	0.82	0.79	0.93	0.83	0.89	0.90
ET	RMSD	"single-site"	0.91 ± 0.31	0.77 ± 0.15	0.74 ± 0.08	0.64 ± 0.05	0.57 ± 0.10	0.55 ± 0.05	0.44 ± 0.03	0.70 ± 0.11
		"all-sites"	0.95 ± 0.29	0.80 ± 0.19	0.75 ± 0.08	0.70 ± 0.08	0.53 ± 0.08	0.59 ± 0.07	0.46 ± 0.03	0.76 ± 0.12
		prior	1.42	1.12	0.85	0.69	0.51	0.57	0.43	0.94
	r	"single-site"	0.81 ± 0.01	0.80 ± 0.04	0.83 ± 0.02	0.86 ± 0.02	0.90 ± 0.01	0.85 ± 0.04	0.92 ± 0.01	0.81 ± 0.06
		"all-sites"	0.81 ± 0.02	0.84 ± 0.03	0.83 ± 0.02	0.86 ± 0.03	0.90 ± 0.01	0.84 ± 0.04	0.92 ± 0.02	0.81 ± 0.07
		prior	0.78	0.84	0.84	0.9	0.91	0.9	0.92	0.88

Table S5. Root mean square deviation (RMSD) averaged among study sites comparing CLASSIC simulations using the prior and optimized plant functional type (PFT)-V_{cmax25} with the corresponding stand-level estimates of gross primary production (GPP) and evapotranspiration (ET). The corresponding estimates are BESS (Li et al., 2021), MODIS-Z (Zhang et al., 2017), MODIS-OD (Running and Zhao, 2021), GLASS (Liang et al., 2021), GOSIF (Li and Xiao, 2019), CLASS (Hobeichi et al., 2020) (Table 1). The units of RMSD are g C m^{-2} day^{-1} for GPP and mm day^{-1} for ET.

Flux	PFT-V_{cmax25}	BESS	MODIS-OD	MODIS-Z	GLASS	GOSIF	CLASS	Average
GPP	"single-site"	1.34	1.12	1.39	0.98	1.23	/	1.22
	"all-sites"	1.19	1.06	1.13	1.10	1.02	/	1.11
	prior	2.93	2.56	3.06	1.78	2.82	/	2.69
ET	"single-site"	0.90	0.56	/	/	/	0.53	0.69
	"all-sites"	0.92	0.58	/	/	/	0.56	0.71
	prior	1.03	0.66	/	/	/	0.64	0.80

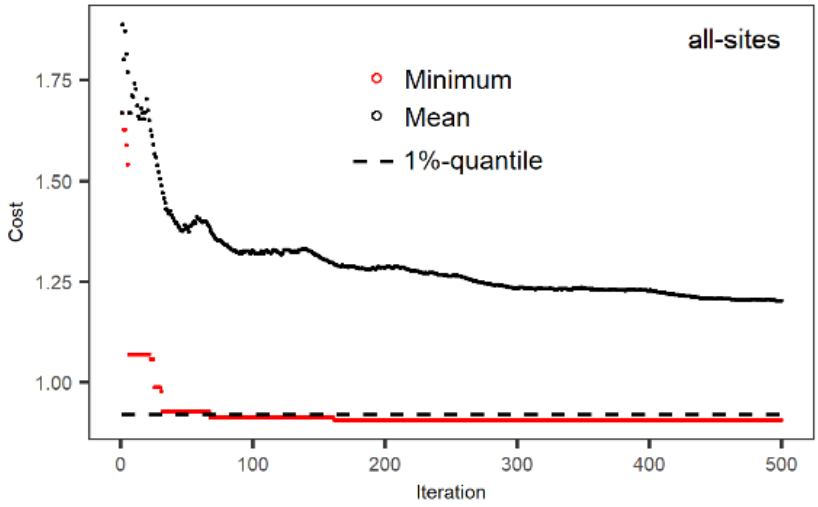

Figure S1. Optimization cost of "all-sites" optimization found before each iteration (Eq. [3] and Sect. 2.3). The dashed line is the 1 % quantile of the minimum cost.

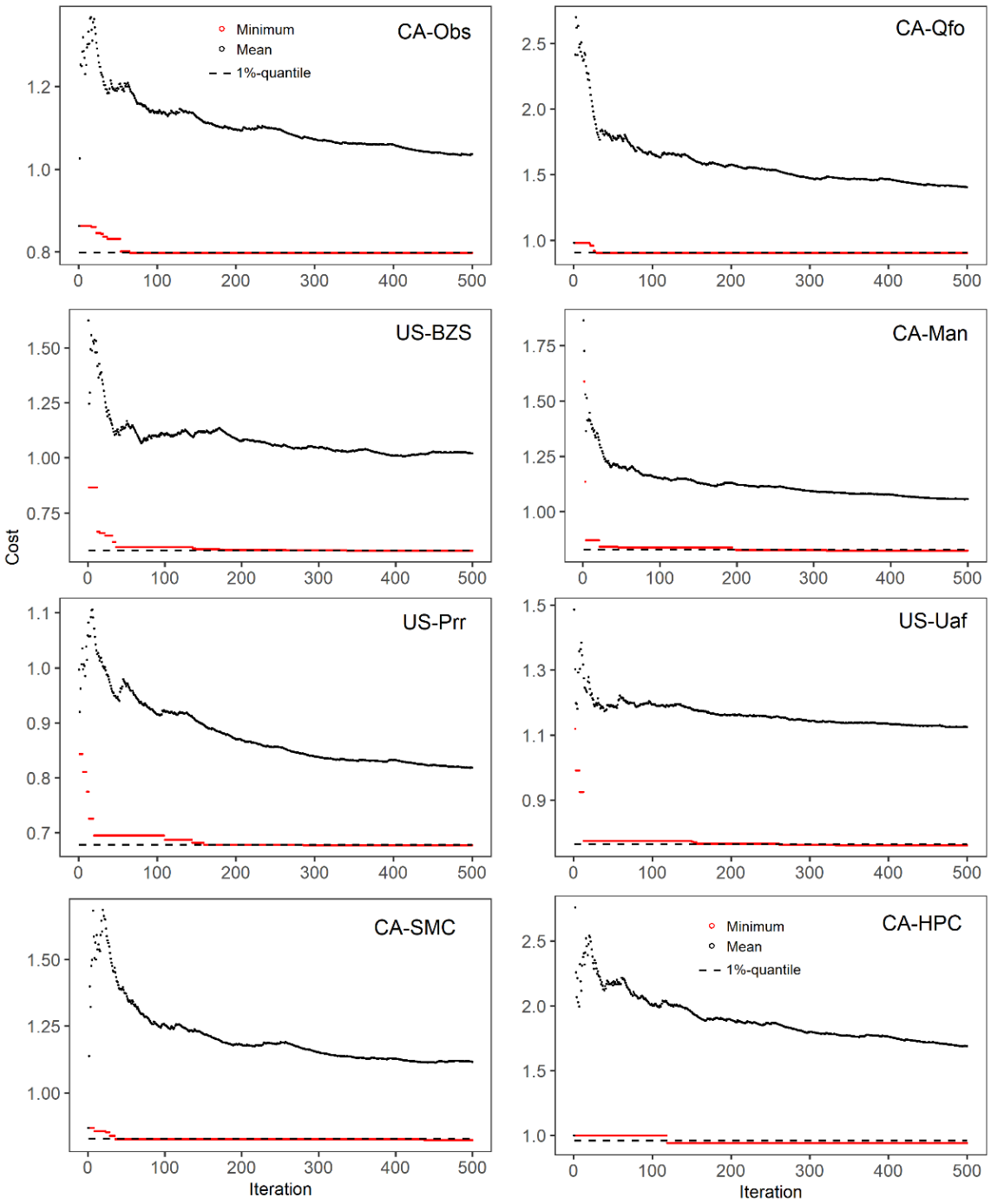

Figure S2. Optimization cost of "single-site" optimizations found before each iteration (Eq. [3] in Sect. 2.3). The dashed line is 1 % quantile of the minimum cost.

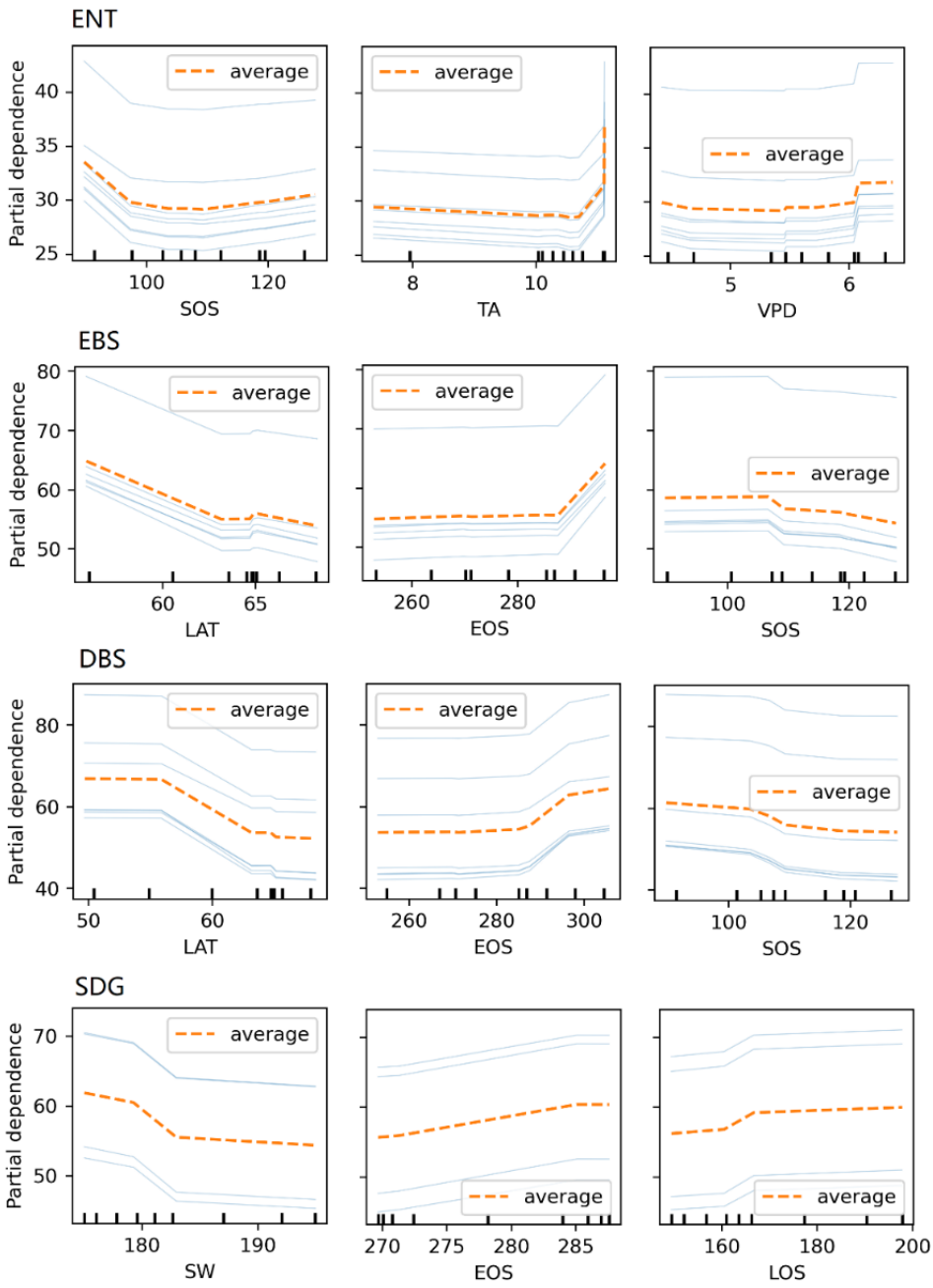

Figure S3. Partial dependence plots of the three most important predictors derived from random forest analyses (Sect. 2.5 and Table 2). Predictors include start (SOS, day of year), end (EOS, day of year), and duration (LOS, days) of growing seasons, latitude (LAT, °), incoming shortwave radiation (SW, W m^{-2}), air temperature (TA, ◦C), and vapor pressure deficit (VPD, hPa). CLASSIC plant functional types are "evergreen needleleaf tree" (ENT), "evergreen broadleaf shrub" (EBS), "deciduous broadleaf shrub" (DBS), and "sedge" (SDG).

References

Bubier, J. L., Smith, R., Juutinen, S., Moore, T. R., Minocha, R., Long, S., and Minocha, S.: Effects of nutrient addition on leaf chemistry, morphology, and photosynthetic capacity of three bog shrubs, Oecologia, 167, 355-368, https://doi.org/10.1007/s00442-011-1998-9, 2011.

Dang, Q.-L., Margolis, H. A., and Collatz, G. J.: Parameterization and testing of a coupled photosynthesis–stomatal conductance model for boreal trees, Tree physiol., 18, 141-153, https://doi.org/10.1093/treephys/18.3.141, 1998.

Heskel, M. A., Bitterman, D., Atkin, O. K., Turnbull, M. H., and Griffin, K. L.: Seasonality of foliar respiration in two dominant plant species from the Arctic tundra: response to long-term warming and short-term temperature variability, Funct. Plant Biol., 41, 287-300, https://doi.org/10.1071/FP13137, 2013.

Hobeichi, S., Abramowitz, G., and Evans, J.: Conserving Land–Atmosphere Synthesis Suite (CLASS), J. Climate, 33, 1821-1844, https://doi.org/10.1175/JCLI-D-19-0036.1, 2020.

Jensen, A. M., Warren, J. M., King, A. W., Ricciuto, D. M., Hanson, P. J., and Wullschleger, S. D.: Simulated projections of boreal forest peatland ecosystem productivity are sensitive to observed seasonality in leaf physiology, Tree Physiol., 39, 556-572, https://doi.org/10.1093/treephys/tpy140, 2019.

Kattge, J. and Knorr, W.: Temperature acclimation in a biochemical model of photosynthesis: a reanalysis of data from 36 species, Plant Cell Environ., 30, 1176-1190, https://doi.org/10.1111/j.1365-3040.2007.01690.x, 2007.

Li, B., Ryu, Y., Jiang, C., Dechant, B., Liu, J., and Yan, Y.: BESS v2.0: A Satellite-driven and Coupled-process Model for Quantifying Global Land-atmosphere Radiation, Energy and CO2 Fluxes since 1982, AGU Fall Meeting 2021, New Orleans, LA, 13-17 December 2021, B15D-1463, 2021.

Li, X. and Xiao, J.: A global, 0.05-degree product of solar-induced chlorophyll fluorescence derived from OCO-2, MODIS, and reanalysis data, Remote Sens., 11, 517, https://doi.org/10.3390/rs11050517, 2019.

Liang, S., Cheng, J., Jia, K., Jiang, B., Liu, Q., Xiao, Z., Yao, Y., Yuan, W., Zhang, X., and Zhao, X.: The global land surface satellite (GLASS) product suite, B. Am. Meteorol. Soc., 102, E323-E337, https://doi.org/10.1175/BAMS-D-18-0341.1, 2021.

Melton, J. R. and Arora, V. K.: Competition between plant functional types in the Canadian Terrestrial Ecosystem Model (CTEM) v.2.0, Geosci. Model Dev., 9, 323-361, https://doi.org/10.5194/gmd-9-323-2016, 2016.

Meyer, G., Humphreys, E. R., Melton, J. R., Cannon, A. J., and Lafleur, P. M.: Simulating shrubs and their energy and carbon dioxide fluxes in Canada's Low Arctic with the Canadian Land Surface Scheme Including Biogeochemical Cycles (CLASSIC), Biogeosciences, 18, 3263-3283, https://doi.org/10.5194/bg-18-3263-2021, 2021.

Pornon, A. and Lamaze, T.: Nitrogen resorption and photosynthetic activity over leaf life span in an evergreen shrub, Rhododendron ferrugineum, in a subalpine environment, New Phytol., 175, 301-310, https://doi.org/10.1111/j.1469-8137.2007.02101.x, 2007.

Qu, B., Sonnentag, O., Roy, A., Melton, J. R., Black, T. A., Amiro, B., Euskirchen, E. S., Ueyama, M., Kobayashi, H., Schulze, C., Gosselin, G. H., and Cannon, A. J.: A boreal forest model benchmarking dataset for North America: a case study with the Canadian Land Surface Scheme including Biogeochemical Cycles (CLASSIC), Zenodo [data set], https://doi.org/10.5281/zenodo.7266010, 2022.

Rayment, M., Loustau, D., and Jarvis, P.: Photosynthesis and respiration of black spruce at three organizational scales: shoot, branch and canopy, Tree Physiol., 22, 219-229, https://doi.org/10.1093/treephys/22.4.219, 2002.

Rogers, A., Serbin, S. P., Ely, K. S., Sloan, V. L., and Wullschleger, S. D.: Terrestrial biosphere models underestimate photosynthetic capacity and CO2 assimilation in the Arctic, New Phytol., 216, 1090-1103, https://doi.org/10.1111/nph.14740, 2017.

Running, S. and Zhao, M.: MOD17A2HGF MODIS/Terra Gross Primary Productivity Gap-Filled 8-Day L4 Global 500 m SIN Grid V061, NASA EOSDIS Land Processes DAAC [data set], https://doi.org/10.5067/MODIS/MOD17A2HGF.061, 2021.

Smith, N. G. and Dukes, J. S.: LCE: Leaf carbon exchange data set for tropical, temperate, and boreal species of North and Central America, Ecology, 98, 2978, https://doi.org/10.1002/ecy.1992, 2017.

Smith, N. G., Keenan, T. F., Colin Prentice, I., Wang, H., Wright, I. J., Niinemets, Ü., Crous, K. Y., Domingues, T. F., Guerrieri, R., and Yoko Ishida, F.: Global photosynthetic capacity is optimized to the environment, Ecol. Lett., 22, 506-517, https://doi.org/10.1111/ele.13210, 2019.

Ueyama, M., Tahara, N., Nagano, H., Makita, N., Iwata, H., and Harazono, Y.: Leaf-and ecosystem-scale photosynthetic parameters for the overstory and understory of boreal forests in interior Alaska, J. Agric. Meteorol., 74, 79-86, https://doi.org/10.2480/agrmet.D-17-00031, 2018.

Wohlfahrt, G., Bahn, M., Haubner, E., Horak, I., Michaeler, W., Rottmar, K., Tappeiner, U., and Cernusca, A.: Inter-specific variation of the biochemical limitation to photosynthesis and related leaf traits of 30 species from mountain grassland ecosystems under different land use, Plant Cell Environ., 22, 1281-1296, https://doi.org/10.1046/j.1365-3040.1999.00479.x, 1999.

Zhang, Y., Xiao, X., Wu, X., Zhou, S., Zhang, G., Qin, Y., and Dong, J.: A global moderate resolution dataset of gross primary production of vegetation for 2000–2016, Sci. Data, 4, 170165, https://doi.org/10.1038/sdata.2017.165, 2017.